Experiments on Axisymmetrically Pulsed Turbulent Jet Flames

Jeffery A. Lovett* and Stephen R. Turns†
Pennsylvania State University, University Park, Pennsylvania

An experimental study of the effects of strong axisymmetric pulsing on a free, vertical turbulent jet diffusion flame is presented. The jet flame was pulsed over the frequency range of 2–1300 Hz with amplitudes ranging from 0.13–0.89 of the centerline jet velocity. Conditionally averaged centerline velocity measurements and flame photographs were obtained to characterize the pulsed jet flames. The centerline evolution of the pulse waveforms was examined and found to be dependent on the pulse frequency; the centerline decay of the pulse amplitude increased with increasing pulse frequency. The visual dimensions of the pulsed flame were also frequency dependent. Significant changes in the local flame structure were observed, which exhibited a constant local nondimensional frequency of about 0.2, consistent with a preferred-mode coupling between the pulsing and the jet flame structure. Several features of the results also suggest a coupling between the forcing and low frequency structure in the outer preheat layer surrounding the jet flame.

Introduction

RADIAL diffusion of mass and momentum in a round jet, which leads to mixing and growth of the jet, is accomplished by the formation and interaction of vortical structures in the surrounding shear layer.[1-4] A considerable amount of research has been conducted to excite these vortex structures in isothermal jets to affect jet growth, mixing, and radiated noise.[1-10] Fewer studies have been reported on excited jet flames, where shear layer mixing controls the rate at which the fuel and oxidant are combined and chemical reaction proceeds. In this study, a turbulent jet diffusion flame was pulsed over a wide range of frequencies and amplitudes to investigate the effects of axisymmetric forcing on mixing and combustion. The results of this work will contribute to an understanding of the role that flow structure plays in jet flames, perhaps ultimately providing a means to actively control flame properties and pollutant emissions actively.

Past research has shown that the structure of the mixing layer in isothermal jets can be altered by axisymmetric excitation.[1-10] When the pulse frequency corresponds to the most unstable frequency for the shear layer, vortex structures are amplified.[1,5,11] Studies by Crow and Champagne,[1] Winant and Browand,[2] Yule,[3] Zaman and Hussain,[5] and others, have applied moderate axisymmetric forcing to air jets enhancing the mixing layer structure. Their results show that significant changes occurred in the structure of the excited jet mixing layer when the Strouhal number, $St = fD/U$, was in the range 0.1–0.9 where D is the initial jet diameter and U the initial jet velocity). This "preferred-mode" scaling may be adventitious in that the shear-layer thickness is the proper characteristic length scale; however, this scaling is generally preserved for laboratory jet flows. The growth of the jet is governed by the interaction and coalescence of vortices generated by instability of the shear layer,[2,5] and several studies[12-14] have demonstrated that vortex interactions and pairing, and hence jet growth, can be controlled with proper excitation. Significant increases in local jet entrainment have been measured in excited jets near the nozzle exit[6-8]; however, the effects of forcing generally vanish by $x/D \simeq 20$.

Bremhorst and Harch[9] studied the effects of pulsing an air jet with large amplitudes ($u_p/U \simeq 1$) and found that local entrainment in the jet was increased by up to three times within $x/D \simeq 17$ for frequencies of 10 and 25 Hz ($St = 0.0071$ and 0.018). Direct measurements of entrainment were made by Vermeulen et al.[10] on a resonantly pulsed air jet and also with very strong forcing ($u_p/U \simeq 2.7$, $St = 0.25$). Here, the effects of forcing were observed as far out as $x/D \simeq 70$, and local entrainment was increased by 200% and 300% in high Reynolds number and transitional jets, respectively. Hence, these studies show that substantial changes in jet growth and entrainment can be affected with high levels of forcing, even at relatively low pulse frequencies.

In jet diffusion flames, hydrodynamic instability of the fuel jet produces a mixing layer structure similar to that observed in cold jets.[15] The reaction zone, however, is located in a thin layer outside of the fuel jet shear layer at low velocities and is located at the edge of the shear layer for higher velocities when jet turbulence is present near the jet exit.[16] A second instability occurs in buoyant diffusion flames in the surrounding region where air is preheated by the flame and is mixed with products diffusing radially outward. This thick buoyancy-driven zone, called the "outer preheat layer," is induced by the high temperature reaction zone and exhibits a low frequency structure ($f = 10$–25 Hz) that is relatively independent of the jet Reynolds number.[15] Inviscid stability analyses for vertical buoyant boundary layers[17-20] have shown that instability occurs over an extremely narrow range of frequency, which for typical hydrocarbon flame temperatures is $f = 6$–17 Hz. This long wavelength structure in the outer preheat layer may be responsible for the low frequency fluctuations observed in diffusion flames,[21,22] which has been observed to persist even after the transition from laminar to turbulent flow, i.e., for Reynolds numbers up to 14.6×10^4.[22] Hence, we see that with a jet flame, buoyancy offers another possibility for interaction between excitation and jet flow structure. A coupling between a shear layer instability and a buoyant instability has been observed by Strawa and Cantwell[23] when axisymmetric excitation was applied to a coflowing laminar jet flame at a frequency of 10 Hz ($St = 0.4$). Vandsburger et al.[24] also used a loudspeaker to excite a laminar flame at a frequency of 16 Hz ($St = 0.27$) and observed the formation of large-scale vortex rings in the flame zone. These studies show that a coupling with buoyant flow structure can be easily obtained in low Reynolds number flames.

Thus, there are two basic modes by which jet flame structure can be excited. Hydrodynamic instabilities in the fuel jet shear layer can be augmented by excitation at $St \approx 0.3$, and

Received Dec. 16, 1988; revision received April 26, 1989.

*Research Assistant, Department of Mechanical Engineering. Member AIAA.

†Associate Professor, Department of Mechanical Engineering. Member AIAA.

second, a coupling with buoyancy-induced structure existing in diffusion flames may be produced with excitation at relatively low frequencies ($f \sim 5$–20 Hz). Since the length scale of the low frequency outer structure is large in comparison to the jet dimensions, interaction with this structure may substantially affect the overall jet flame. In the present study, strong axisymmetric forcing has been applied to a turbulent jet flame in which both buoyancy and initial jet momentum are important. Forcing was applied over the frequency range of 2–1300 Hz to determine if coupling with naturally occurring instabilities can alter flame structure.

Experimental Methods

The measurements presented here were made in a vertical unconfined propane jet diffusion flame having an exit Reynolds number of 1×10^4. The jet flame was surrounded by a 61×61 cm cross-section screen enclosure to mitigate disturbances from the room air, and a forced-draft hood centered above the flame exhausted the combustion products from the laboratory. The burner, enclosure, and hood were mounted to a carriage that could be traversed in two orthogonal directions to probe the flame with the stationary laser Doppler velocimetry (LDV) system.

The flame burner consisted of two concentric stainless steel tubes with the propane fuel gas flowing through the 76-mm-long central tube ($D = 3.86$ mm i.d., 5.57 mm o.d.) and hydrogen stabilizer gas flowing through the annular space between the tubes (outside tube: 7.75 mm i.d., 8.80 mm o.d.). The inside diameter of the cental tube, D, was used as the characteristic length in the dimensionless parameters herein. A 30-W, 100-mm-diam loudspeaker and fairing were mounted coaxially beneath the fuel tube, as illustrated in Fig. 1. Motion of the loudspeaker cone modulated the fuel jet exit velocity. The fuel gas entered the burner through two inlets above the loudspeaker and then passed into the fuel tube through an ASME nozzle. The loudspeaker was surrounded by a 1440-cm^3 enclosure that was connected to the top side of the loudspeaker to eliminate static pressure loading on the speaker cone. The loudspeaker was driven by a sine-wave generator, decade attenuator, and power amplifier as shown schematically in Fig. 2.

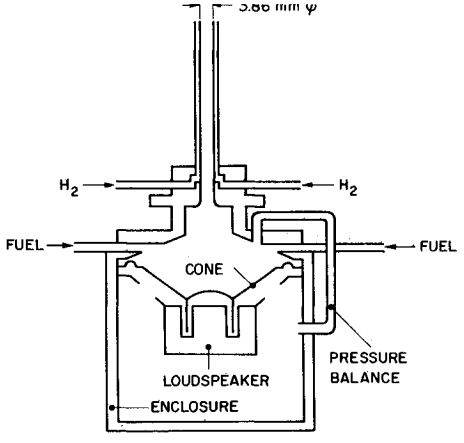

Fig. 1 Pulsed flame burner.

The propane and hydrogen gas flow rates were controlled using precision rotameters that were calibrated and operated with the inlet pressure held constant at a high pressure. The gas flow was throttled to the desired pressure after the flow meter. This configuration suppressed any upstream pressure fluctuations associated with pulsing the jet and maintained constant gas density inside the flow meter. The hydrogen mass flow rate used was 0.2% of the propane mass flow rate. An investigation of the stability characteristics of pulsed flames[25] showed that axisymmetric pulsing did not destabilize the flame.

Axial velocity measurements were made in the flame using a dual-beam, backscatter LDV system with frequency shifting. The configuration of the experimental instrumentation is illustrated in Fig. 2. The complete system is capable of measuring two velocity components, but only the 514-nm laser line was used to measure the axial velocity in this study. A 3.75x beam expander and 750-mm focusing lens were employed which resulted in estimated probe volume dimensions of 1.64 mm × 0.089 mm and a beam crossing angle of 6.20 deg. The LDV data were acquired on a microcomputer equipped with parallel ports. The signal from the LDV counter processor was also used to latch a 100-kHz clock providing time-resolved measurements. The clock was retriggered by the pulse signal source; hence, the acquired LDV data time was proportional to the phase of the pulse.

To facilitate the LDV measurements, the fuel gas was seeded with nominal 0.05 μm alumina particles using a cyclone seeder. Since no outer air flow was provided, the air entrained by the flame did not contain seed particles, which could cause serious seeding bias in LDV measurements obtained where significant outside air has been entrained. On the jet centerline, however, the intermittency is very low, and seeding bias is not expected to be severe. Examination of the temporal distribution of LDV data samples referenced to the pulse showed that the data were uniformly distributed throughout the pulse period (except for velocity bias caused by the mean pulse velocity). Hence, no obvious intermittency was correlated with the pulse on the centerline suggesting that seeding bias was not serious in the present measurements. This finding is also supported by the results of Dibble et al.[26] in a study of LDV

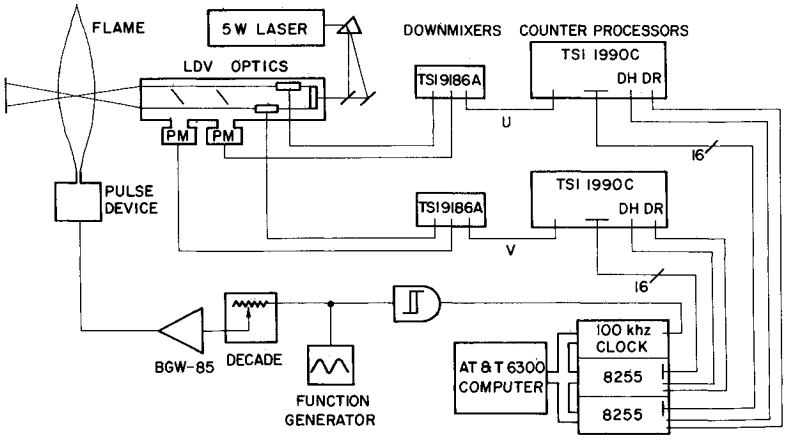

Fig. 2 Schematic of the experimental instrumentation.

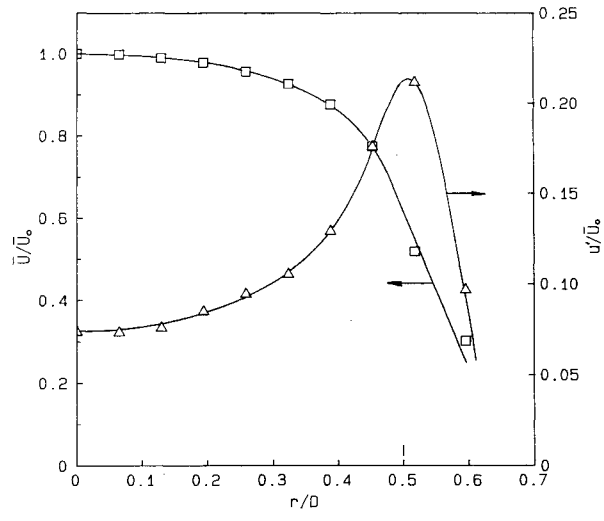

Fig. 3 Radial distribution of the axial mean velocity and turbulence intensity for the unpulsed jet flame at $x/D = 0.26$, $Re = 1 \times 10^4$.

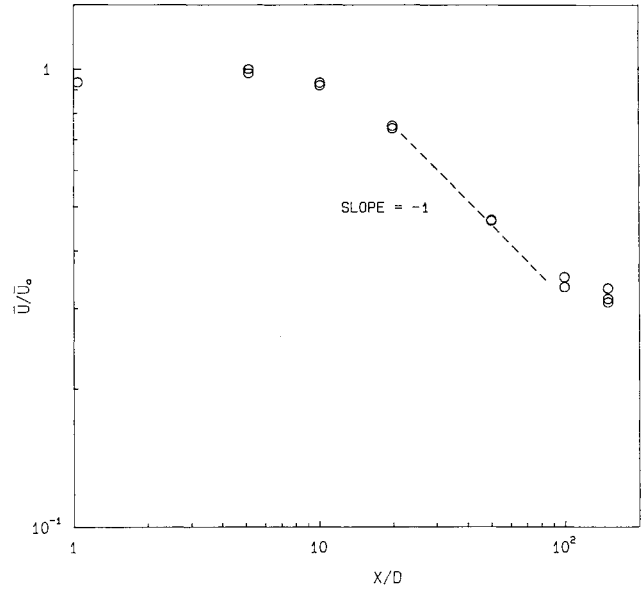

Fig. 4 Centerline distribution of the mean velocity for the unpulsed jet flame.

seeding bias in a hydrogen jet flame at $Re = 1.9 \times 10^4$, where no measurable bias occurred on the jet axis for $x/D \leq 50$. Histograms of the LDV data were routinely examined, and particle seeding and signal processing were carefully controlled to insure that spurious samples were minimized and that the nonuniformly disturbed submicron soot particles existing in the flame were not counted by the LDV system. No bias corrections were applied to the data because of the uncertain validity of corrections for unsteady flows with large fluctuation levels. The one-dimensional velocity weighting suggested by McLaughlin and Tiederman[27] was investigated and found to have an insignificant effect on the mean velocity measurements for both the unpulsed and pulsed conditions.

Results and Discussion

Axial Velocity Measurements

Unpulsed Flame

Axial velocity measurements were made to characterize the unpulsed jet diffusion flame. Radial distributions of the mean axial velocity component $\bar{U}$ and the root-mean-square of the velocity fluctuations u' at the jet exit are shown in Fig. 3. These measurements were made 1 mm ($x/D = 0.26$) downstream from the jet exit, the closest position obtainable because of the LDV beam angle. The mean velocity was uniform over the central portion of the jet, and a strong shear layer existed at the edge of the jet. The jet flame centerline mean exit velocity $\bar{U}_0$ was 13.5 m/s, and the centerline turbulence intensity u' was $0.078\bar{U}_0$. The axial decay of the centerline mean velocity for the unpulsed jet flame is shown in Fig. 4. The mean velocity decayed approximately as x^{-1} for $x/D > 20$ which generally agrees with data for isothermal jets,[28] a propane flame,[29] and a hydrogen flame.[30] Buoyancy generated by combustion acts to decrease the decay rate for $x/D \geq 100$. Centerline turbulence intensities for the unpulsed jet flame were found to agree with the measurements of Driscoll et al.[31] for a hydrogen flame and with Jeng[32] for a methane flame.

Phase-average Velocities

Measurements of the pulse wave in the pulsed jet flame were made by decomposing the centerline axial velocity measurements into a long-time mean velocity $\bar{U}$, a conditionally averaged pulse velocity u, and a fluctuation about the pulse u:

$$U(x,t) = \bar{U}(x) + \tilde{u}(x,t) + u(x,t)$$

Using this decomposition, the pulse velocity, $\tilde{u}$ is zero-mean and periodic with a period $T = 1/f$, where f is the pulse frequency. The basic pulse wave is then given by the phase-averaged velocity $\tilde{u}$, measured by sorting the LDV data into bins according to the phase with respect to the driving pulse. The data samples within each pulse bin were analyzed to determine the mean and root-mean-square (rms) fluctuation for the conditional samples in that bin. For each test condition, a total of 20,000 LDV data samples were acquired. The flow was considered to be statistically stationary, and many pulse periods lapsed during data collection. The pulse period was separated into 30 equally spaced phase bins, so each bin contained on the order of 600–700 data samples. Experiments indicated that 30 bins provided optimum resolution of the pulse wave shape with good repeatability (±3% in the bin average). An example of the measured pulse is shown in Fig. 5, where the mean with rms velocity in each phase bin is plotted as a function of the phase time normalized by the pulse period. The pulse wave was clearly reconstructed by the conditional pulse velocity > $\tilde{u}$. In all cases, the conditional rms velocity was approximately proportional to the absolute mean velocity for that phase bin, i.e., $\bar{U} + \tilde{u}$.

In the following discussion, the peak amplitude of the pulse A is defined as the one-sided peak amplitude with respect to the long-time mean velocity; for example, $A = 8$ m/s in Fig. 5. The peak amplitude measured at the jet exit ($x = 1$ mm) is denoted by A_0. Experiments showed that large amplitude modulation of the jet could be achieved over a frequency range of 2–100 Hz. Equal pulse amplitudes were obtained at various pulse frequencies by measuring the pulse amplitude at the jet exit and precisely varying the input power to the loudspeaker. Significant pulse amplitudes also were achieved at two empirically determined acoustic resonant frequencies for the burner; viz., 310 and 1300 Hz. The matrix of test conditions listed in Table 1 was evaluated to investigate the independent effects of pulse frequency and pulse amplitude. In general, five amplitude settings were used covering a range of $A_0 = 4$–12 m/s, corresponding to 30–89% modulation of the centerline velocity, respectively. The highest frequency condition, $f = 1300$ Hz, is particularly interesting in that $St = 0.37$, a condition similar to those found to cause excitation of the mixing layer in isothermal jets.[1-4]

Examination of the pulse shapes measured at the jet exit showed that the basic characteristics of the initial pulse were very similar, regardless of the pulse frequency and amplitude. The phase-normalized shapes of the exit pulse wave for several pulse frequencies at an initial amplitude of $A_0 = 4$ m/s are

shown in Fig. 6, which shows that all of the pulse waveforms were sinusoidal and of equal amplitude. At higher pulse amplitudes, some distortion of the mean shapes was observed, but, in general, the pulse shapes were quite similar. This distortion was at least partly due to velocity bias which existed at high pulse amplitudes ($A/\bar{U} \geq 0.75$); i.e., the large difference in velocity between the high and low peak of the pulse affected the distribution of samples in the phase bins. Nevertheless, these results showed that the shapes of the initial waveforms were similar for all test conditions and that constant amplitude cross-conditions had been obtained. The exit pulse characteristics were also measured at several off-axis positions at each frequency to check for any significant nonuniformity in the pulse. These measurements indicated that the pulse amplitude for $f \leq 100$ Hz diminished off axis in roughly the same manner as the mean velocity distribution (cf. Fig. 3), indicating that the pulse was uniform and in phase over most of the jet exit plane. Although the waveforms did become distorted in the shear layer at the edge of the jet, the phase and period of the waveforms was unchanged. Measurements also indicated that the pulse for the two resonant frequencies of 310 and 1300 Hz was much less uniform; hence, these measurements are considered qualitative until more detailed radial measurements are obtained. Off-axis measurements of the pulse at several downstream positions were consistent with the findings at the jet exit. Although these off-axis measurements may be biased because the outer flow was not seeded, the measurements did confirm that the mean pulse shape was axisymmetric. The data also showed that the propagation velocity of the pulse waves was roughly equal to the mean local flow velocity.

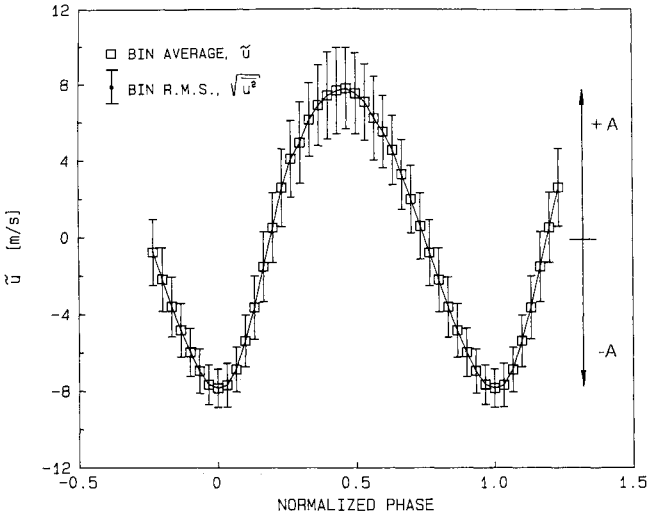

Fig. 5 Example of pulse measured in a jet flame using the bin-sorting technique, measured on the jet centerline at $x/D = 0.26$ with $f = 20$ Hz and $A_0 = 8$ m/s.

Pulse Decay

A fundamental measure of the evolution of the pulse as it propagated downstream in the jet is the change in the peak amplitude A. In Fig. 7, normalized peak amplitudes measured in the pulsed flame are shown as functions of the downstream distance. The data show that at $x/D = 5$, the pulse amplitude was slightly increased followed by rapid decay of the amplitude downstream. The dashed lines in Fig. 7 illustrate that the pulse decayed more rapidly with increasing pulse frequency. Only pulses at the lowest frequencies were sustained out to x/D 100. In all cases, the relative decay rate of the pulse peak was stronger than the decay of the mean velocity in the unpulsed jet flame, shown as a solid line in Fig. 7. Similar results for the centerline decay of the peak amplitude were observed

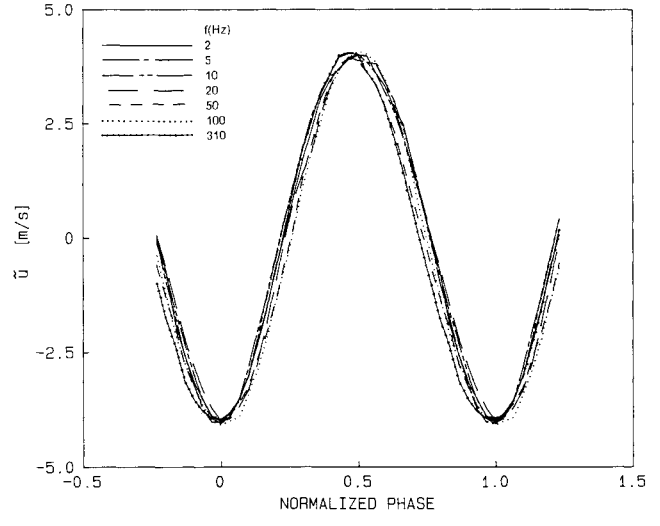

Fig. 6 Phase-normalized pulse waveforms at the jet exit for $A_0 = 4$ m/s.

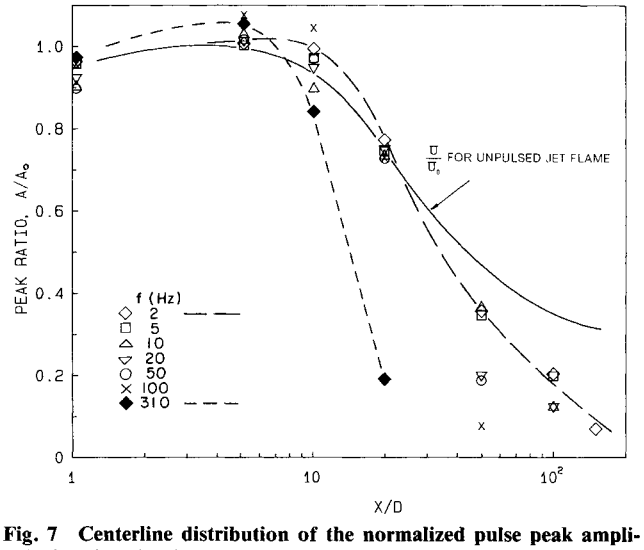

Fig. 7 Centerline distribution of the normalized pulse peak amplitude for $A_0 = 4$ m/s.

Table 1 Pulsed flame test conditions, $Re = 1 \times 10^4$, $\bar{U}_0 = 13.5$ m/s, $D = 3.86$ mm

Frequency, f (Hz)	Amplitude, A_0 (m/s)	$A_0/\bar{U}_0$	$St = fD/\bar{U}_0$
2	4, 6, 8	0.296, 0.444, 0.593	0.57×10^{-3}
5	4, 6, 8, 10, 12	0.296, 0.444, 0.593, 0.741, 0.889	1.43×10^{-3}
10	4, 6, 8, 10, 12	0.296, 0.444, 0.593, 0.741, 0.889	2.86×10^{-3}
20	4, 6, 8, 10, 12	0.296, 0.444, 0.593, 0.741, 0.889	5.72×10^{-3}
50	4, 6, 8, 10, 12	0.296, 0.444, 0.593, 0.741, 0.889	14.3×10^{-3}
100	4, 6, 8	0.296, 0.444, 0.593	28.6×10^{-3}
310	4	0.296	0.089
1300	1.7	0.126	0.372

for the other four initial pulse amplitudes tested, indicating that the basic response of the jet flame was independent of the pulse amplitude. Comparing the results for different pulse amplitudes did show, however, that the peak amplitude decay rate increased slightly with increasing initial amplitude. The reduced peak amplitude at $x/D=1$ was apparently due to an adjustment of the flow very near the jet exit which has been observed in similar studies.[1,33]

From Fig. 7, we can see that the maximum pulse amplitude at $x/D=10$ occurred for $f=100$ Hz, and at $x/D=100$, the strongest pulse occurred for $f=2$–5 Hz. Therefore, over an increase of one decade in axial distance, the frequency with the strongest local response decreased approximately two decades. This frequency behavior $f\sim x^{-2}$ suggests that the response of the pulsed jet flame depends on a local Strouhal number, suggested also, as we shall see, by visual observations. A local Strouhal number based on the jet width can be estimated using the scaling relationships found for cold jets.[28] The mean velocity $\bar{U}$ decays as x^{-1}; the jet width W grows as x; therefore, the local nondimensional frequency behaves as $St_w = fW/\bar{U} \sim fx^2$. Hence, the frequency behavior observed for the pulse peak amplitude appears to be consistent with a constant local Strouhal number scaling.

The centerline measurements for the pulsed jet flames showed that the long-time mean velocity was generally unaffected by forcing for $f<100$ Hz; hence, this forcing did not appear to create a substantial effect on jet entrainment or dissipation. However, for pulse frequencies of $f \geq 100$ Hz, the centerline long-time mean velocity was significantly reduced for $x/D>10$, indicating that overall jet entrainment was affected.

Pulse Shapes

The downstream evolution of the pulse shape was also found to be dependent on the pulse frequency. Examination of the pulse as it propagated downstream showed that a steepening of the waveform occurred during the acceleration phase such that the wave shape approached a saw-tooth waveform. This phenomenon is shown in Fig. 8, where the phase-normalized pulse waveforms measured at $x/D=20$ are plotted for several pulse frequencies. These data clearly show that the steepening of the pulse increased with increasing pulse frequency. The complete set of results also showed that the strength of this steepening effect increased with pulse amplitude but also that an amplitude threshold existed for wave steepening; i.e., once the pulse amplitude became relatively small ($A<4$ m/s), no wave steepening occurred, and the wave simply attenuated as it propagated downstream. The observed wave steepening is similar to nonlinear acoustic wave propagation[34]; however, in our case, the pulse wave propagates at roughly the local flow velocity rather than at the sound speed. The acceleration or steepening of the pulse wave may be caused by buoyancy produced by locally increased mixing and combustion on a length scale smaller than the pulse wavelength. The accelerating phase of the pulse in an Eulerian reference frame corresponds to a region where $d\tilde{U}/dx<0$ in a Lagrangian system. The strong deceleration existing in this region may enhance the local turbulence and mixing, which in turn results in a larger volumetric heat release, locally accelerating the flow. This effect would become stronger with increasing pulse frequency because the pulse wavelength decreases producing yet larger velocity gradients in the flow. This wave steepening phenomenon warrants further study.

At all pulse frequencies except for $f=5$ Hz, the pulse generally steepened and decayed as it propagated downstream. For example, Fig. 9 shows the downstream evolution of a pulse with $f=20$ Hz and $A_0=12$ m/s. For high amplitude forcing at a frequency of 5 Hz, however, a unique feature in the pulse evolution was observed and is shown in Fig. 10. Under these conditions, repeatable small-scale perturbations in the waveform occurred downstream during the acceleration phase of the pulse. These disturbances on the centerline may be induced

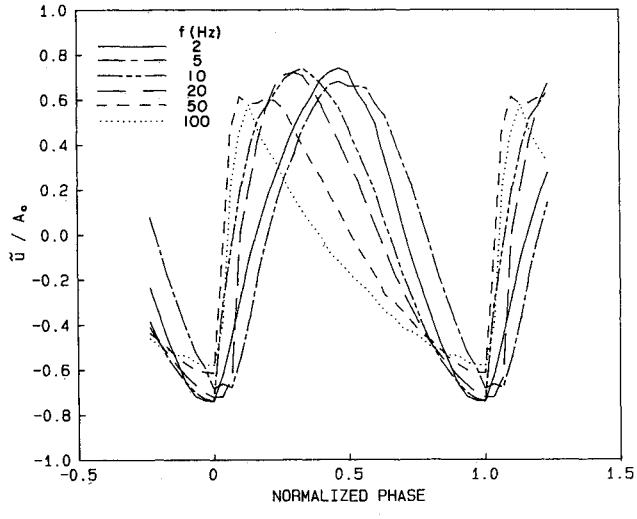

Fig. 8 Phase-normalized pulse waveforms measured at $x/D=20$ for $A_0=8$ m/s.

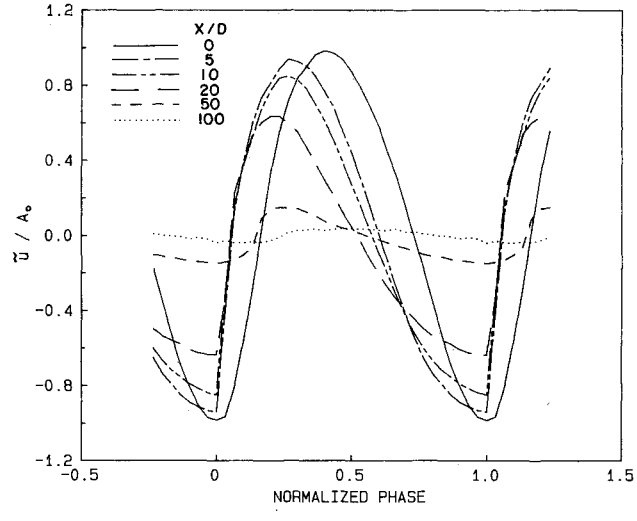

Fig. 9 Centerline evolution of a pulse with $f=20$ Hz and $A_0=12$ m/s.

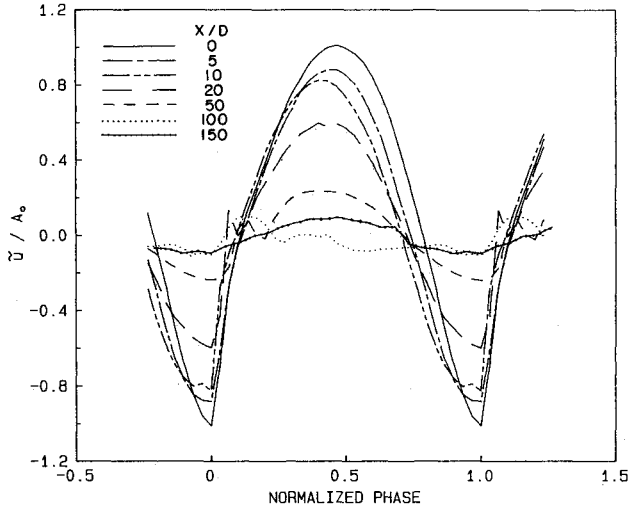

Fig. 10 Centerline evolution of a pulse with $f=5$ Hz and $A_0=12$ m/s.

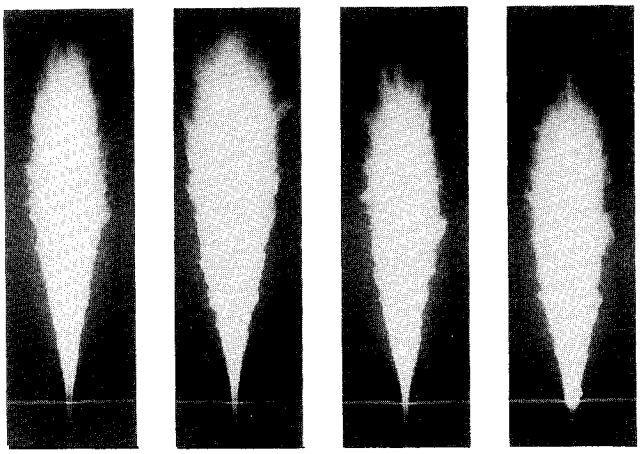

a) Unpulsed flame | b) $f=5$ Hz, $A_0=0.59\bar{U}_0$ | c) $f=20$ Hz, $A_0=0.59\ U$ | d) $f=100$ Hz, $A_0=0.59\ \bar{U}_0$

Fig. 11 Unpulsed and pulsed luminous jet flames.

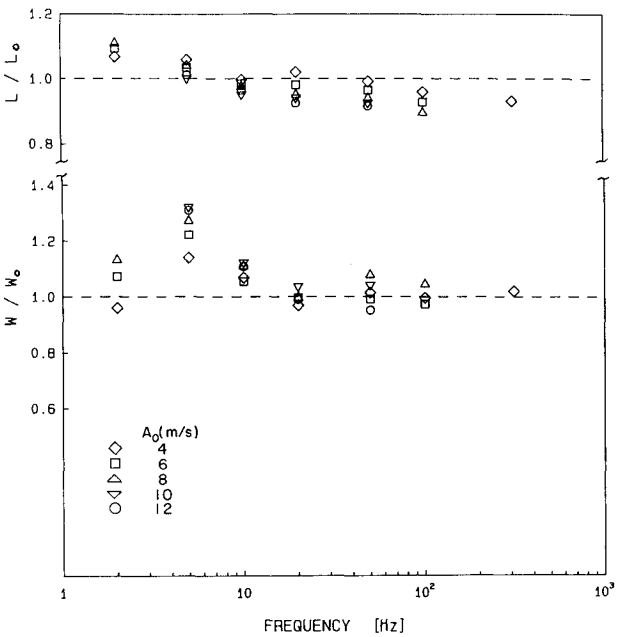

Fig. 12 Average length and maximum width of pulsed flames as a function of the pulse frequency.

by structures in the flame enhanced by a subharmonic interaction between the forced jet at $f = 5$ Hz and low frequency structure in the outer preheat layer occurring at $f \approx 10$–20 Hz.

The centerline pulse waveforms measured for the two resonant frequencies of 310 and 1300 Hz were generally undistorted, presumably because the peak amplitudes were relatively low. The measurements indicated that the pulse for $f = 310$ Hz completely disappeared by $x/D \simeq 50$, and forcing at $f = 1300$ Hz vanished by $x/D \simeq 20$. From visual observations of the luminous flame, it appeared that strong excitation of the shear layer near the jet exit was obtained with forcing at $f = 1300$ Hz $St = 0.37$, $A_0/\bar{u}_0 = 0.13$); the flame zone near the jet exit ($0 < x/D < 10$) was strongly disturbed as indicated by the appearance of increased turbulence and holes in the flame sheet. The downstream structure of the flame, however, appeared to be unaffected by forcing at $f = 1300$ Hz. Hence, these results showed that excitation of jet flame structure near the jet exit for $St = 0.37$ disappeared quickly, similar to the results for isothermal jets.

Flame Photographs

Overall Dimensions

The visual flame, caused by soot incandescence, provides a valuable visualization of jet flame structure. Measurements of the average flame dimensions were made from photographs obtained with a 35-mm camera and an exposure time of 8 s. Figure 11 shows example photographs of unpulsed and pulsed jet flames, where changes in the average flame shape produced by forcing can easily be seen. The vertical field of view in the photographs is about 1 m, and the length of the unpulsed flame (Fig. 11a) was about 0.84 m ($L_0/D = 218$), which agrees with reported flame length measurements.[35] The average length and width of the luminous flame were measured to examine the effect of pulsing on the overall flame dimensions. The average flame length L and the maximum flame width W normalized by the corresponding length and width of the unpulsed flame L_0 and W_0 are plotted as functions of the pulse frequency for several pulse amplitudes in Fig. 12. Each data point represents the average of two or more independent measurements. The data indicate that the average length and width of the pulsed jet flame were dependent on the pulse frequency; whereas the pulse amplitude affected only the magnitude of the change. The average flame length was increased for $f = 2$ and 5 Hz, and the flame length was decreased for $f \geq 10$ Hz. The increase in flame length at low frequencies may result because the jet flame momentarily behaves like an impulsively started jet that exhibits reduced mixing and growth compared with a steady jet.[36] The overall flame width was substantially increased for low pulse frequencies of $f = 2$–10 Hz.

Local Widening

The photographs presented in Fig. 11 also show that a local widening of the flame was produced by forcing, which moved progressively toward the jet exit with increasing pulse frequency. For example, in Fig. 11b, the flame width was considerably increased over the top half of the flame; in Fig. 11c, the flame width was increased about 25% of the way up from the jet exit; and in Fig. 11d, a relatively large increase in the flame width can be seen very near the jet exit at the bottom of the photograph. Measurements of the local flame dimensions at the position where this flame widening was apparent are listed in Table 2. The axial location where substantial widening of the flame was observed, L', is tabulated along with the width of the flame W', and the corresponding width of the unpulsed flame W_0'. These data clearly show that the axial location corresponding to the coupling between forcing and the flame structure L' decreased with increasing pulse frequency. The local flame width was increased by 30% to over 200% compared to the unpulsed flame. Furthermore, the measurements showed that the axial location of flame widening was independent of the pulse amplitude, and that little additional widening of the flame occurred for pulse amplitudes above $A_0 \approx 8$ m/s, suggesting an amplitude saturation had been reached. The local nondimensional frequency associated with the flame widening St_w based on the local flame width and the centerline mean velocity, is also listed in Table 2. In light of the subjectivity in measuring the flame dimensions, the data show that the interaction occurred at a constant local Strouhal number of approximately 0.2. The Strouhal number for $f = 2$ Hz is lower because the interaction occurred near the end of the flame where the flame luminosity ended and thus introduces a bias to the observed flame structure. Similarly, measurements very close to the jet exit were difficult to obtain because of low luminosity there, which explains the larger Strouhal number for $f = 310$ Hz. Also included in Table 2 are comparable measurements made from a pulsed flame with $Re = 2 \times 10^4$ obtained using a piston-cylinder driver.[25] With a frequency variation of over 8-1, the local Strouhal number was, again, essentially constant and nearly equal to 0.2. Hence, these data suggest that the constant Strouhal number coupling observed was not strongly influenced by the Reynolds number.

High-speed Motion Pictures

A series of high-speed motion pictures were obtained of the unpulsed and pulsed luminous jet flames to examine the instantaneous flame structure and flow dynamics associated with pulsing. The photographs were taken with an exposure of 0.2 ms and a frame rate of 2000 pictures/s. For the unpulsed flame, instantaneous photographs showed that combustion occurs essentially over the entire time-averaged visible length of the flame. The flame structure of a pulsed jet flame is shown in Fig. 13, which shows a complete pulse cycle with $f=10$ Hz and $A_0 \approx 0.8\bar{U}_0$. The bottom of the frame corresponds to the jet exit, and the vertical field of view is approximately 1 m. The sequence was constructed by compiling successive frames at 45-deg phase intervals. The immediate observation is that, with forcing, the reaction was organized into discrete regions with a length scale of the order of the jet width, which convect downstream. The structure of these coherent reaction regions was largely axisymmetric and significantly wider than the unpulsed jet flame; hence, these structures were likely responsible for the flame widening observed in the long-exposure flame photographs. The luminous intensity in the discrete large-scale structures was larger than the intensity of the unpulsed flame. Similar motion pictures with $f=2.5$ Hz showed that the reaction was again separated into large coherent regions, and the separation spacing was unchanged (i.e., the spacing was again about two-thirds of the frame). Furthermore, motion pictures of a pulsed flame with $Re=6\times10^4$ also indicated the same separation distance between the reaction zones. Hence, these results suggest that a range of low pulse frequencies can couple with the flow structure resulting in large structures with a single wavelength that is largely independent of the jet Reynolds number. Motion pictures of flames pulsed at high frequencies ($f \geq 50$ Hz) indicated that the reaction was not separated into discrete regions, and this coupling was lost. These effects are consistent

Table 2 Local flame dimensions associated with flame widening

f,Hz	$A_0/\bar{U}_0$	W_0'/D	W'/D	W'/W_0'	L'/D	$\bar{U}/\bar{u}_0$	$St_w=fW'/\bar{U}$
2	0.593	21.2	34.5	1.18	196	0.302	0.065
5	0.593	32.4	44.5	1.37	174	0.308	0.207
5	0.889	33.1	48.0	1.45	170	0.309	0.222
10	0.593	23.5	33.8	1.44	88.9	0.356	0.271
10	0.889	23.5	33.5	1.43	88.9	0.356	0.269
20	0.593	12.5	16.4	1.31	49.8	0.467	0.201
20	0.889	10.1	13.5	1.33	40.9	0.521	0.148
50	0.593	7.47	8.18	1.10	30.2	0.607	0.193
50	0.889	8.54	11.0	1.29	36.3	0.555	0.283
100	0.593	3.56	7.83	2.20	14.2	1.00	0.224
310	0.296	3.20	7.83	2.44	12.5	1.00	0.694
$Re=2\times10^4$, using piston-cylinder device[25]							
10	0.803	22.6	37.7	1.67	69.5	0.397	0.136
82	0.803	4.34	12.2	2.80	17.4	0.776	0.184

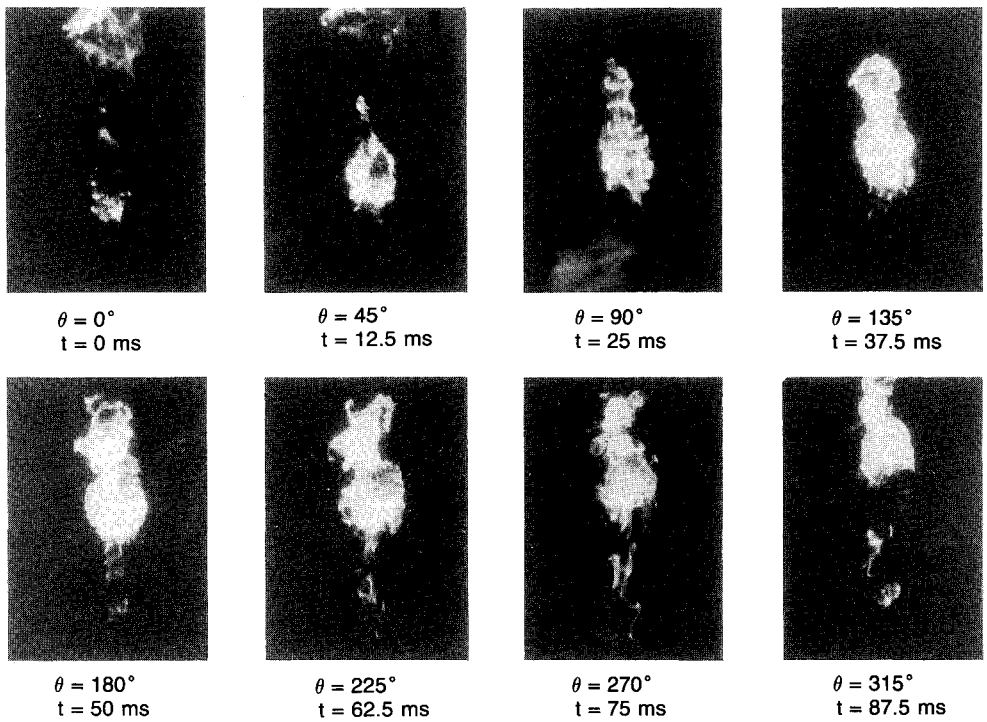

Fig. 13 High-speed motion-picture sequence of a pulsed flame cycle with $Re=2\times10^4$, $f=10$ Hz, and $A_0\approx0.8\bar{U}_0$.

with the hypothesis that a subharmonic coupling is created with the vortex structure in the outer preheat layer.

Conclusions

The results of this study show that a turbulent jet flame is sensitive to axisymmetric pulsing of the fuel stream and that the effects observed are largely frequency dependent. The jet flame structure responds locally to a frequency that decreases with downstream distance approximately as x^{-2}, consistent with a local Strouhal number coupling. The pulse amplitude on the jet axis decays more rapidly as the pulse frequency and initial pulse amplitude are increased, and an amplitude saturation is suggested by the results. Detailed measurements of the pulse waveform show that the pulse wave steepens as the pulse propagates downstream, possibly due to the influence of buoyancy. This acceleration of the flow increases strongly with increasing pulse frequency and amplitude. The steepening effect does not appear to progress once the pulse amplitude becomes sufficiently small. Several unique features were observed at a pulse frequency of $f = 5$ Hz, indicating an interaction with the pulse that was not observed at the other pulse frequencies tested. Furthermore, only low frequency forcing ($f \leq 20$ Hz) could be detected at large distances downstream ($x/D \geq 100$).

The effects of pulsing cause a significant increase in the local width of the luminous flame as a result of the generation of large-scale structures in the flow. Coupling between the forcing and the jet flame occurs at an axial position such that the local Strouhal number based on the jet width is constant, i.e., $St_w \simeq 0.2$. This interaction did not appear to be a strong function of the jet Reynolds number. Low frequency forcing separates the reaction in the flame into discrete large-scale regions with a spacing that is essentially independent of the jet Reynolds number and pulse frequency. These results are consistent with the hypothesis that low frequency pulsing of the jet causes a subharmonic coupling with structure in the outer preheat layer surrounding a jet flame. Pulse frequencies of $f = 2$ and 5 Hz also produce an increase in the overall flame dimensions, and higher frequency forcing ($f > 10$ Hz) reduces the overall flame length. High frequency and high amplitude ($u_p \sim \bar{U}$) forcing increases the net turbulent mixing in the jet flame, significantly reducing the overall flame dimensions.

Pulsing the jet flame at a frequency corresponding to an exit Strouhal number of $St = 0.37$ excited the shear layer surrounding the jet flame near the exit; however, similar to observations with isothermal jets, the pulse disappeared by $x/D = 20$, and no substantial effect on the overall jet flame was observed.

Acknowledgments

This work was supported by the Gas Research Institute under Contract 5086-260-1308, with Program Manager J. A. Kezerle, and by the National Science Foundation through Equipment Grant CBT-8704795.

References

[1]Crow, S. C. and Champagne, F. H., "Orderly Structure in Jet Turbulence," *Journal of Fluid Mechanics,* Vol. 48, 1971, pp. 547-591.

[2]Winant, C. D. and Browand, F. K., "Vortex Pairing: The Mechanism of Turbulent Mixing-Layer Growth at Moderate Reynolds Number," *Journal of Fluid Mechanics,* Vol. 63, 1974, pp. 237-255.

[3]Yule, A. J., "Large-Scale Structure in the Mixing Layer of a Round Jet," *Journal of Fluid Mechanics,* Vol. 89, 1978, pp. 413-432.

[4]Hussain, A. K. M. F., "Coherent Structures and Turbulence," *Journal of Fluid Mechanics,* Vol. 173, 1986, pp. 303-356.

[5]Zaman, K. B. M. Q. and Hussain, A. K. M. F., "Vortex Pairing in a Circular Jet under Controlled Excitation: Part 1. General Jet Response," *Journal of Fluid Mechanics,* Vol. 101, 1980, pp. 449-491.

[6]Favre-Marinet, M. and Binder, G., "Structure des Jets Pulsants," *Journal de Mecanique,* Vol. 18, 1979, pp. 355-394.

[7]Parikh, P. G. and Moffat, R. J., "Mixing Improvement in a Resonantly Pulsed, Confined Jet," *Fluid Mechanics of Combustion Systems,* ASME, New York, 1981, pp. 251-256.

[8]Sarohia, V. and Bernal, L. P., "Entrainment and Mixing in Pulsatile Jets," *Third Symposium on Turbulent Shear Flows,* University of California, Davis, CA, 1981, pp. 11.30-11.35.

[9]Bremhorst, K. and Harch, W. II.,"Near Field Velocity Measurements in a Fully Pulsed Subsonic Air Jet," *Turbulent Shear Flows I,* Springer-Verlag, Berlin, 1979, pp. 480-500.

[10]Vermeulen, P. J., Ramesh, V., and Yu, W. K., "Measurements of Entrainment by Acoustically Pulsed Axisymmetric Air Jets," *Journal of Engineering Gas Turbines and Power,* Vol. 108, 1986, pp. 479-484.

[11]Michalke, A., "On the Spatially Growing Disturbances in an Inviscid Shear Layer," *Journal of Fluid Mechanics,* Vol. 23, 1965, pp. 521-544.

[12]Zaman, K. B. M. Q. and Hussain, A. K. M. F., "Turbulence Suppression in Free Shear Flows by Controlled Excitation," *Journal of Fluid Mechanics,* Vol. 103, 1981, pp. 133-159.

[13]Oster, D. and Wygnanski, I., "The Forced Mixing Layer between Parallel Streams," *Journal of Fluid Mechanics,* Vol. 123, 1982, pp. 91-130.

[14]Ho, C. M. and Huang, L. S., "Subharmonics and Vortex Merging in Mixing Layers," *Journal of Fluid Mechanics,* Vol. 119, 1982, pp. 443-473.

[15]Yule, A. J., Chigier, N. A., Ralph, S., Boulderstone, R., and Ventura, J., "Combustion-Transition Interaction in a Jet Flame," *AIAA Journal,* Vol. 19, 1981, pp. 752-760.

[16]Roquemore, W. M., Chen, L. D., Seaba, J. P., Tschen, P. S., Goss, L. P., and Trump, D. D., "Jet Diffusion Flame Transition to Turbulence," *Physics of Fluids,* Vol. 30, No. 9, 1987, p. 2600.

[17]Gebhart, B., "Instability, Transition, and Turbulence in Buoyancy-Induced Flows," *Annual Review of Fluid Mechanics,* Vol. 5, 1973, pp. 213-246.

[18]Dring, R. P. and Gebhart, B., "A Theoretical Investigation of Disturbance Amplification in External Laminar Natural Convection," *Journal of Fluid Mechanics,* Vol. 34, 1968, pp. 551-564.

[19]Gebhart, B. and Mahajan, R., "Characteristic Disturbance Frequency in Vertical Natural Convection Flow," *International Journal of Heat and Mass Transfer,* Vol. 18, 1975, pp. 1143-1148.

[20]Buckmaster, J. and Peters, N., "The Infinite Candle and its Stability – A Paradigm for Flickering Diffusion Flames," *Twenty-First Symposium (International) on Combustion,* The Combustion Institute, Pittsburgh, PA, 1986, pp. 1829-1836.

[21]Grant, A. J. and Jones, J. M., "Low Frequency Diffusion Flame Oscillations," *Combustion and Flame,* Vol. 25, 1975, pp. 153-160.

[22]Ballantyne, A. and Bray, K. N. C., "Investigations into the Structure of Jet Diffusion Flames using Time-Resolved Optical Measuring Techniques," *Sixteenth Symposium (International) on Combustion,* The Combustion Institute, Pittsburgh, PA, 1977, pp. 777-785.

[23]Strawa, A. W. and Cantwell, B. J., "Visualization of the Structure of a Pulsed Methane-Air Diffusion Flame," *Physics of Fluids,* Vol. 28, 1985, pp. 2317-2320.

[24]Vandsburger, U., Lewis, G., Seitzman, J. M., and Allen, M. G., "Flame-Flow Structure in an Acoustically Driven Jet Flame," Western States Section/The Combustion Institute Fall Meeting, University of Arizona, Paper 86-19, 1986.

[25]Lovett, J. A., Turns, S. R., and Merkle, C. L., "Stability Characteristics of Pulsed Jet Diffusion Flames," Central States Section/The Combustion Institute Spring Meeting, Argonne National Laboratories, Argonne, IL, 1987, pp. 304-309.

[26]Dibble, R. W., Hartmann, V., Schefer, R. W., and Kollmann, W., "Conditional Sampling of Velocity and Scalars in Turbulent Flames Using Simultaneous LDV-Raman Scattering," *Experiments in Fluids,* Vol. 5, 1987, pp. 103-113.

[27]McLaughlin, D. K. and Tiederman, W. G., "Biasing Correction for Individual Realization of Laser Anemometry Measurements in Turbulent Flows," *Physics of Fluids,* Vol. 16, 1973, pp. 2082-2088.

[28]Wygnanski, I. and Fiedler, H., "Some Measurements in the Self-Preserving Jet," *Journal of Fluid Mechanics,* Vol. 38, 1969, pp. 577-580.

[29]Szekely, G. A., Jr., "Experimental Evaluation of a Locally Homogeneous Flow Model of Spray Combustion," M. S. Thesis, Department of Mechanical Engineering, Pennsylvania State Univ., University Park, 1980.

[30]Glass, M. and Bilger, R. W., "The Turbulent Jet Diffusion Flame in a Co-flowing Stream—Some Velocity Measurements," *Combustion Science and Technology,* Vol. 18, 1978, pp. 165–177.
[31]Driscoll, J. F., Schefer, R. W., and Dibble, R. W., "Mass Fluxes $\overline{\rho' u'}$ and $\overline{\rho' v'}$ Measured in a Turbulent Nonpremixed Flame," *Nineteenth Symposium (International) on Combustion,* The Combustion Institute, Pittsburgh, PA, 1982, pp. 477–485.
[32]Jeng, S. M., "An Investigation of the Structure and Radiation Properties of Turbulent Buoyant Diffusion Flames," Ph.D. Thesis, Department of Mechanical Engineering, Pennsylvania State Univ., University Park, 1984.
[33]Lepicovsky, J., "Laser Velocimeter Measurements of Large-Scale Structures in a Tone-Excited Jet," *AIAA Journal,* Vol. 24, Jan. 1986, pp. 27–31.
[34]Beyer, R. T., *Nonlinear Acoustics in Fluids,* Van Nostrand Reinhold, New York, 1984, p. 118.
[35]Becker, H. A. and Liang, D., "Visible Length of Vertical Free Diffusion Flames," *Combustion and Flame,* Vol. 32, 1978, pp. 115–138.
[36]Kovasznay, L. S. G., Hajime, F., and Lee, R. L., "Unsteady Turbulent Puffs," *Advances in Geo-Physics,* Vol. 18B, 1974, pp. 253–263.